A quantum chemical study of nitric oxide reduction by ammonia (SCR reaction) on V2O5 catalyst surface

ARTICLE *in* CATALYSIS TODAY · DECEMBER 2006

Impact Factor: 3.89 · DOI: 10.1016/j.cattod.2006.07.033

4 AUTHORS, INCLUDING:

Alper Uzun
Koc University
32 PUBLICATIONS **440** CITATIONS
SEE PROFILE

Isik Onal
Middle East Technical University
63 PUBLICATIONS **641** CITATIONS
SEE PROFILE

Available online at www.sciencedirect.com
ScienceDirect
Catalysis Today 118 (2006) 268–278
CATALYSIS TODAY
www.elsevier.com/locate/cattod

A quantum chemical study of nitric oxide reduction by ammonia (SCR reaction) on V_2O_5 catalyst surface

Sezen Soyer [a], Alper Uzun [a], Selim Senkan [b], Isik Onal [a,*]

[a] *Department of Chemical Engineering, Middle East Technical University, Ankara 06531, Turkey*
[b] *Department of Chemical Engineering, University of California, Los Angeles, CA 90095, USA*

Available online 1 September 2006

Abstract

The reaction mechanism for the selective catalytic reduction (SCR) of nitric oxide by ammonia on (0 1 0) V_2O_5 surface represented by a $V_2O_9H_8$ cluster was simulated by means of density functional theory (DFT) calculations performed at B3LYP/6-31G** level. The computations indicated that SCR reaction consisted of three main parts. For the first part, ammonia activation on V_2O_5 was investigated. Ammonia was adsorbed on Brønsted acidic V–OH site as NH_4^+ species by a non-activated process with an exothermic relative energy difference of 28.65 kcal/mol. Lewis acidic ammonia interactions were also considered and they were found to be energetically unfavorable. Therefore, it is concluded that the SCR reaction on (0 1 0) vanadium oxide surface is initiated favorably by the Brønsted acidic ammonia adsorption. The second part of the SCR reaction consists of the interaction of nitric oxide with the pre-adsorbed ammonia species to eventually form nitrosamide (NH_2NO) species. The rate limiting step for this part as well as for the total SCR reaction can be identified as NH_3NHO formation with a high activation barrier of 43.99 kcal/mol; however, it must be cautioned that only an approximate transition state was obtained for this step. For the last part, gas phase decomposition of NH_2NO and decomposition of this species on catalyst surface were both considered. Gas phase decomposition of NH_2NO was found to have high activation barriers when compared with the NH_2NO decomposition on $V_2O_9H_8$ cluster surface. NH_2NO decomposition on this cluster was achieved by means of a push–pull hydrogen transfer mechanism between the active V=O and V–OH groups.

Keywords: Selective catalytic reduction; SCR; NO reduction; NH_3; Quantum chemical calculations; Density functional theory; DFT; V_2O_5

1. Introduction

Selective catalytic reduction (SCR) of nitric oxide by ammonia over V_2O_5/TiO_2 based catalysts is the most technically advanced post-combustion technology capable of reducing NO_x emissions to extremely low levels mandated in many areas of the world.

Although there are numerous experimental studies carried out on SCR reaction over vanadium-based catalysts, a complete elucidation of the reaction mechanism has not been achieved. It is generally believed that the reaction occurs through an Eley-Rideal type mechanism in which ammonia is adsorbed on the vanadium-based catalyst in the first step, and the reaction then proceeds with the activation of nitric oxide from the gas phase [1–13]. However, the adsorption mode of the ammonia over the catalytic surface is still unclear. Inomata et al. [1,2] suggested that the active site for the ammonia activation is the Brønsted acidic V_s–OH site adjacent to V^{5+}=O site as a result of TPD and IR studies. Ammonia is strongly adsorbed on this site as NH_4^+. By means of the isotopic transient studies with oxygen-18 and nitrogen-15, Janssen et al. [3,4] considered the V=O species to be the active site that was easily reduced. According to this study, ammonia was adsorbed on this site as V–ONH_2 by reducing the adjacent V=O site to V–OH. Nan-Yu Topsøe [5–7] suggested that predominantly Brønsted acid sites (V–OH) were present and active on the surface of oxidized V_2O_5 for the ammonia activation reaction, in agreement with the proposal of Gasior et al. [8]. By means of isotopic labeling studies using $^{18}O_2$, $^{15}NH_3$, ^{15}NO, and $^{15}N^{18}O$, Ozkan et al. [9,10] suggested that ammonia adsorbs on the pairs of V–OH groups, leading to the formation of surface ammonium ion species. In contrast to these studies, Ramis et al. [11–13] suggested that Brønsted acidity is not a necessary requirement for SCR activity. Ammonia is activated for SCR by coordination over Lewis acidic sites on TiO_2 as well and this activated ammonia is easily transformed to amide NH_2 species by the hydrogen abstraction.

* Corresponding author. Tel.: +90 312 210 2639; fax: +90 312 210 1264.
E-mail address: ional@metu.edu.tr (I. Onal).

0920-5861/$ – see front matter © 2006 Elsevier B.V. All rights reserved.
doi:10.1016/j.cattod.2006.07.033

Gilardoni et al. [14,15] theoretically proposed that at the end of the nitric oxide interaction reaction with the pre-adsorbed NH_4^+ species over V_2O_5 surface as V_2O_9H cluster, NH_2NO species form in the gas phase; it then undergoes a series of isomerization reactions in the gas phase to give reaction products nitrogen and water. Similarly, Anstrom et al. [16,17] theoretically investigated the role of V_2O_5 in the reaction of adsorbed NH_4^+ species with nitric oxide by using a vanadium oxide cluster containing four vanadium atoms with a Brønsted acidic V–OH site. Yin et al. [18] performed periodic first-principles DFT calculations for the mechanism of SCR of NO by NH_3 over V_2O_5 (0 1 0) surface and suggested the presence of two synergetic functional groups as: a hydroxyl group (V–OH) containing vanadyl oxygen responsible for the formation of NH_4^+ species, and a V=O group for the activation of the NH_4^+ formed on the other site. Besides these studies, there have also been quite a few theoretical studies employing the cluster approach on vanadia/titania models [19–23].

The objective of the present study is to elucidate the full sequence of reaction steps including intermediates and transition state geometries, and the energetics for the SCR of nitric oxide by ammonia on the surface of V_2O_5. Density functional theory (DFT) computations were performed to obtain the transition state and equilibrium geometry structures at each step. Vibration frequency calculations were also done for optimized geometries and compared with experimental FTIR data. The effect of TiO_2 support on the SCR reaction is currently being investigated and will be submitted for publication soon.

2. Surface model and calculation method

Quantum chemical calculations employing DFT [24] were conducted to investigate the energetics of the reaction of ammonia with nitric oxide over a finite vanadium oxide cluster representing the (0 1 0) surface of V_2O_5. This cluster approach is a well known and successful approach applied in quantum chemical calculations [25,26]. DFT calculations were conducted using Becke's [27,28] three-parameter hybrid method involving Lee et al. [29] correlation functional (B3LYP) formalism. The basis set employed in the DFT calculations was 6-31G** provided in SPARTAN'04 (Wavefunction Inc.) [30,31].

A $V_2O_9H_6$ cluster was first obtained from (0 1 0) surface by cutting out V_2O_9 part and saturating all of the peripheral oxygen atoms by hydrogen atoms. This cluster size is significantly larger than the molecular sizes of ammonia, nitric oxide, and SCR products, so that the chemisorption properties of the surfaces should be minimally altered. Moreover, Michalak et al. [32] showed that this size of the cluster gives a very reasonable description of the local electronic structure near the V_2O_5 (0 1 0) surface. A similar approach was also applied by Anstrom et al. [16,17].

Both Lewis and Brønsted acid sites of the vanadia cluster were studied following the above methods for ammonia adsorption. Neutral clusters are employed in DFT computations. Lewis acidic $V_2O_9H_8$ cluster is formed by adding two hydrogen atoms to the peripheral oxygen atoms of the $V_2O_9H_6$ cluster to obtain a neutral cluster (Fig. 1). For the Brønsted acidic ammonia adsorption calculations a Brønsted acidic site (V1-O1H) is created by adding one H atom to the V1-O1 site of the $V_2O_9H_6$ cluster to provide charge neutrality (Fig. 2). The location of the Brønsted acidic site is selected as doubly bonded O1 atom since this site was considered as the most active site of the V_2O_5 cluster in literature [14–16,33,34]. The optimized geometries of the Lewis and the Brønsted acidic clusters used in the DFT calculations are shown in Figs. 1 and 2, respectively. In all of the calculations, V1, O1, V2, O1′, H1 atoms and the bridge oxygen atom (O2), were relaxed while the rest of the cluster atoms were kept fixed.

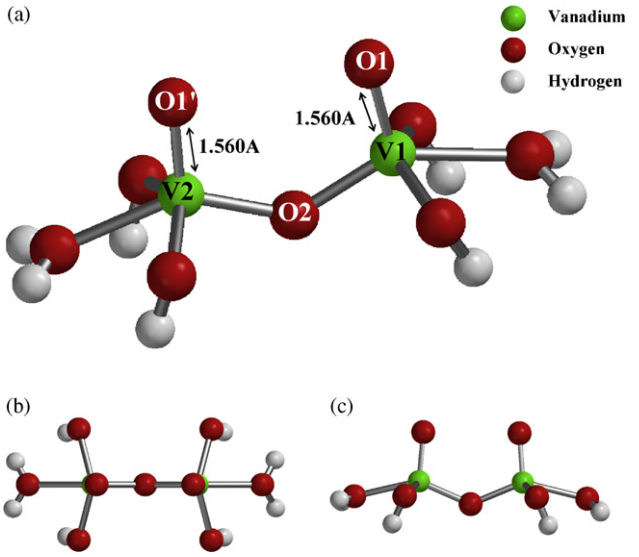

Fig. 1. (a) The structure of the optimized Lewis acidic $V_2O_9H_8$ cluster, (b) top view, and (c) side view.

The following general computational procedure was followed: initially, both the cluster and the adsorbing molecules are fully optimized geometrically by means of the equilibrium geometry calculations. Then, the adsorbing molecule is located over the active site of the cluster at a selected distance and a

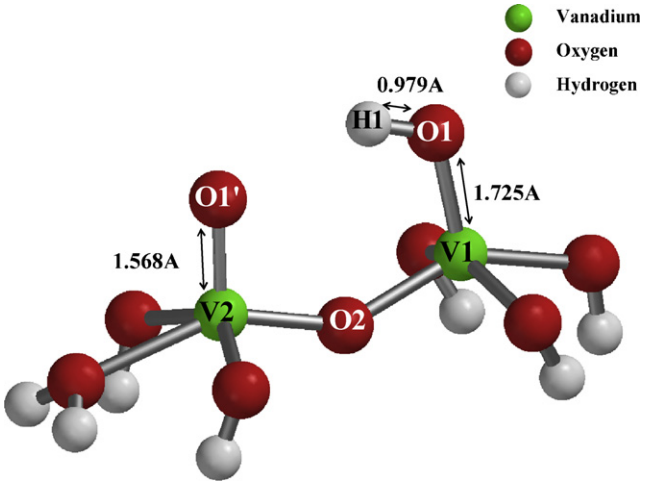

Fig. 2. The structure of the optimized Brønsted acidic $V_2O_9H_8$ cluster.

coordinate driving calculation is performed by selecting a reaction coordinate in order to obtain the variation of the relative energy with a decreasing reaction coordinate to get an energy profile as a function of the selected reaction coordinate distance. Single point equilibrium geometry calculations were also performed where necessary by locating the adsorbing molecule in the vicinity of the catalytic cluster.

The relative energy is defined as:

$$\Delta E = E_{\text{system}} - (E_{\text{cluster}} + E_{\text{adsorbate}})$$

where E_{system} is the calculated energy of the given geometry containing cluster and the adsorbing molecule at any interatomic distance, E_{cluster} the energy of the cluster itself and $E_{\text{adsorbate}}$ is that of the adsorbing molecule.

After having obtained the energy profile for the desired reaction, the geometry with the minimum energy on the energy profile is re-optimized by means of the equilibrium geometry calculations to obtain the final geometry for the reaction. For the calculated final geometry, vibration frequencies and atomic charges are computed by single point energy calculations. Furthermore, from the energy profile, the geometry with the highest energy is taken as the input geometry for the transition state geometry calculations. Starting from these geometries, the transition state structures with only one negative eigenvalue in Hessian matrix are obtained. If a successful transition state geometry cannot be achieved, the geometry with the maximum energy in the energy profile is reported as the approximate transition geometry.

3. Results

Before performing mechanism calculations over the catalytic surface represented by the $V_2O_9H_8$ cluster, the reactants (NH_3 and NO) were initially optimized by means of the equilibrium geometry calculations. Then the computational procedure described in Section 2 was applied for investigating the SCR reaction mechanism, and through these calculations it has been established that SCR reaction consists of three main parts:

- Part I: Brønsted acidic ammonia adsorption reaction.
- Part II: NH_2NO formation reactions.
- Part III: NH_2NO decomposition reactions.

3.1. Part I: initiation step

It is generally agreed that the SCR reaction is initiated with the activation of ammonia which is strongly adsorbed over the catalytic surface, and it then proceeds by the interaction of NO with pre-adsorbed ammonia, suggesting an Eley-Rideal type mechanism as mentioned in Section 1 [1–13]. Therefore, ammonia activation over the (0 1 0) V_2O_5 catalytic surface was considered as the initiation reaction of the SCR of nitric oxide by ammonia. Ammonia activation may occur through two different mechanisms: ammonia can be adsorbed on vanadium catalyst either through Lewis-type interaction as molecularly adsorbed ammonia, or over a Brønsted acidic site as ammonium ion. These two possibilities were considered separately and a comparison between them was made to select the most favorable one.

3.1.1. Lewis acidic ammonia adsorption

Ammonia adsorption through a Lewis acidic interaction is one of the possible activation modes of ammonia over V_2O_5 surface. This interaction type was investigated over the optimized Lewis Acidic $V_2O_9H_8$ cluster (Fig. 1). For this type of ammonia activation mode, coordinate driving calculations were performed by selecting four different reaction coordinates as the distances between: (1) one of the hydrogen atoms of ammonia and O1 site of the $V_2O_9H_8$ cluster, (2) one of the hydrogen atoms of ammonia and V site of the $V_2O_9H_8$ cluster, (3) the nitrogen of the ammonia and the O1 site of the cluster, and (4) the nitrogen atom of the ammonia and O1 site of the cluster. Since the total energy of the system shows a continuous rise as ammonia gets close to O1 or V active sites in the resultant energy profiles for all of the above calculations, it is concluded that Lewis acidic NH_3 adsorption is an unfavorable reaction for the initiation step.

3.1.2. Brønsted acidic ammonia adsorption

Another possible activation mode of ammonia on V_2O_5 catalytic surface is the adsorption over Brønsted acidic V1-O1H1 site of the $V_2O_9H_8$ cluster as shown in Fig. 2. In order to investigate the Brønsted acidic ammonia adsorption over the cluster, the distance between the nitrogen atom of ammonia and Brønsted acidic O1-H1 site of the cluster is selected as the reaction coordinate for a coordinate driving calculation and decreased in a stepwise manner. The system is taken as neutral and with singlet spin multiplicity in this calculation. The energy profile obtained accordingly shows that ammonia activation over Brønsted acidic V–OH site occurs through a non-activated process. The equilibrium geometry of this interaction is given in Fig. 3 where ammonia is adsorbed over the Brønsted acidic site of the cluster symmetrically forming NH_4 species over the catalytic surface with an exothermic energy of −28.65 kcal/mol with respect to $V_2O_9H_8$ cluster and NH_3 (g) molecule. For this geometry, single point energy calculations are carried out to obtain vibration frequencies and Mulliken charges. The calculated vibration frequencies which are contributed by symmetric and asymmetric bending and stretching frequencies of NH_4, are compared with the experimental values available in the literature as given in Table 1. Moreover, the Mulliken charge calculated for the equilibrium geometry of the Brønsted acidic NH_3 adsorption reaction is +0.787e.

As a result of these calculations, it is concluded that the SCR reaction is initiated more favorably by the strong non-activated ammonia adsorption mechanism on Brønsted acidic V–OH site and the adsorbed ammonia forms NH_4^+ ion over the catalytic surface. Since the favorable activation mode of the ammonia over the catalytic surface was Brønsted acidic adsorption, the second part of the SCR reaction was investigated by introducing nitric oxide to the final geometry of the Brønsted acidic ammonia adsorption.

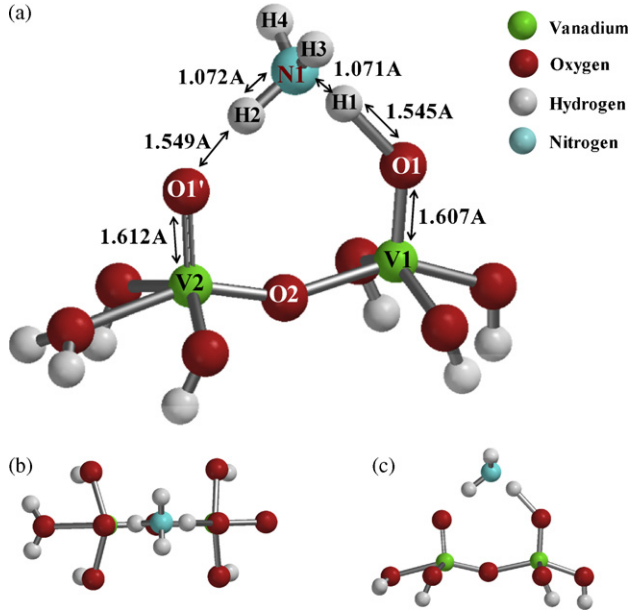

Fig. 3. (a) Equilibrium geometry of Brønsted acidic NH_3 adsorption on $V_2O_9H_8$ cluster, (b) top view, and (c) side view.

3.2. Part II: formation of NH_2NO species

As the second part of the SCR reaction, nitric oxide interaction with the pre-adsorbed ammonia species is investigated. For this purpose a coordinate driving calculation is performed by considering the distance between the nitrogen atom (N1) of the NH_4^+ ion formed at the end of part I and that of NO (N2) as the reaction coordinate. The system is considered as neutral and with doublet spin multiplicity for all of the calculations in this part. An approximate transition state and the equilibrium geometry are derived by use of an energy profile for the formation of NH_3NHO adduct as shown in Fig. 4(a) and (b), respectively. This reaction step has a high activation barrier of 43.99 kcal/mol.

After the formation of NH_3NHO species, in order to achieve the migrations of H1 and H2 atoms of this species towards the O1 and O1′ sites of the cluster two separate reaction coordinates of O1–H1 and O1′–H2 are selected to perform a coordinate driving calculation. As a result of this calculation NH_2NO is formed with an exothermic relative energy of 14.08 kcal/mol.

Table 1
Comparison of the calculated vibration frequency (cm^{-1}) data for the optimized geometry of Brønsted acidic NH_3 adsorption reaction with experimentally obtained ones

Frequency (cm^{-1})	This work	Experimental literature
NH_4 bend. (asym.)	1392 (unscaled), 1514 (scaled by 1.0873)	1425 [11], 1417 [5]
NH_4 bend. (sym.)	1528 (unscaled), 1661 (scaled by 1.0873)	1680 [11], 1670 [5]
NH_4 stret. (asym.)	2593 (unscaled), 2819 (scaled by 1.0873)	2850 [11]
NH_4 stret. (sym.)	2754 (unscaled), 2994 (scaled by 1.0873)	3000 [11]

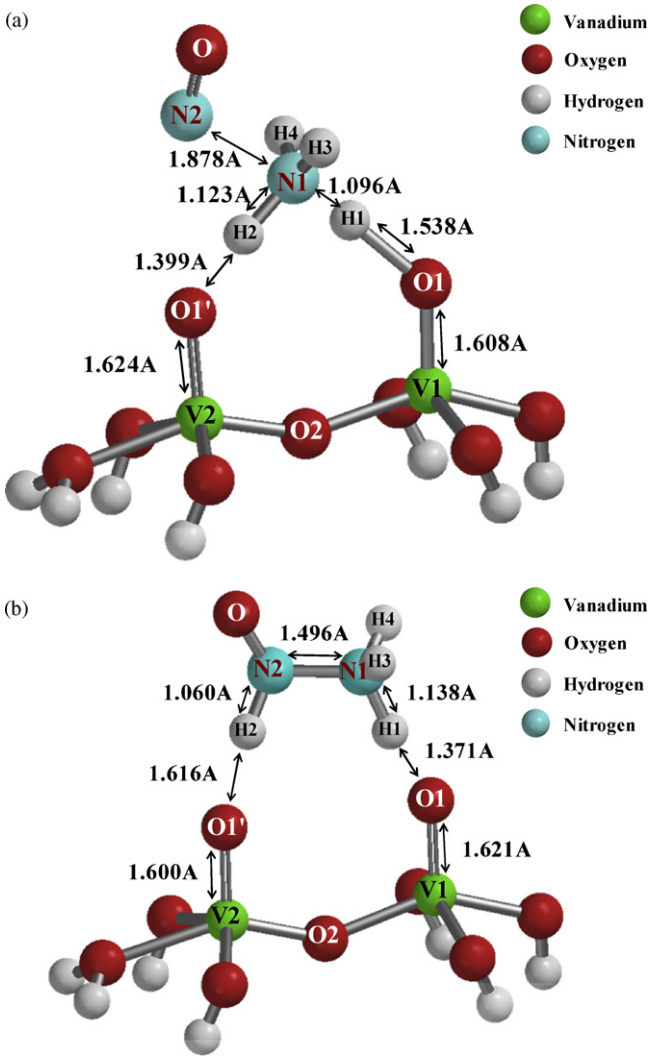

Fig. 4. (a) Approximate transition state and (b) equilibrium geometry obtained for the interaction of gas phase NO with the pre-adsorbed NH_4 species to form NH_3NHO adduct.

Both of the oxygen sites of the cluster are now saturated with hydrogen atoms. An approximate transition state and the equilibrium geometry for this reaction step are given in Fig. 5(a) and (b), respectively. A summary of the reaction steps of parts I and II are illustrated in Fig. 6 in terms of relative potential energies. The relative energy values in this part are calculated with respect $V_2O_9H_8$ cluster and gas phase energies of ammonia and nitric oxide at infinite separation.

3.3. Part III: decomposition of NH_2NO species

In this part, decomposition of nitrosamide species formed previously is further considered both on a new cluster surface and in gas phase as described below.

3.3.1. Decomposition of NH_2NO species on V_2O_5 surface

The reaction steps of this part are given in Fig. 7 as a relative potential energy diagram. The relative energy values in this part are calculated with respect to $V_2O_9H_8$ cluster and gas phase

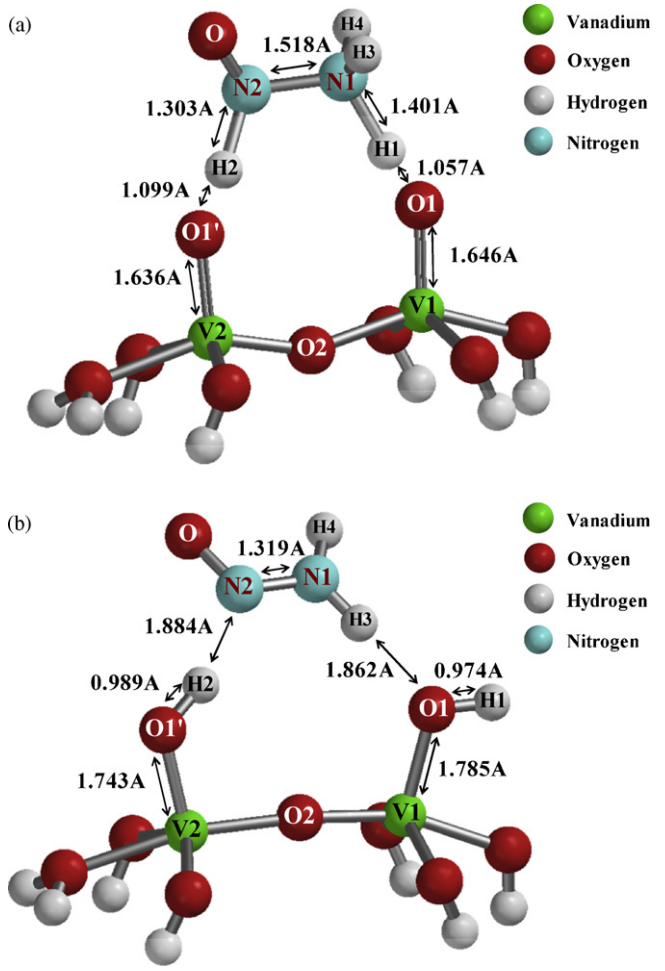

Fig. 5. (a) Approximate transition state and (b) equilibrium geometry for NH_2NO formation reaction from NH_3NHO adduct.

energy of NH_2NO species. The reaction series for the decomposition of NH_2NO species on the cluster start with the re-adsorption of nitrosamide species on a new Brønsted acidic $V_2O_9H_8$ cluster by a single point equilibrium geometry

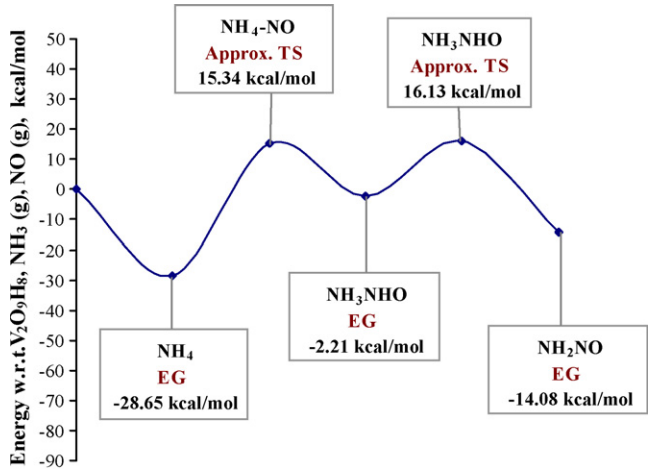

Fig. 6. Potential energy profile for the first and second parts of SCR reaction (approximately TS represents the approximate transition states, while EG stands for the equilibrium geometries).

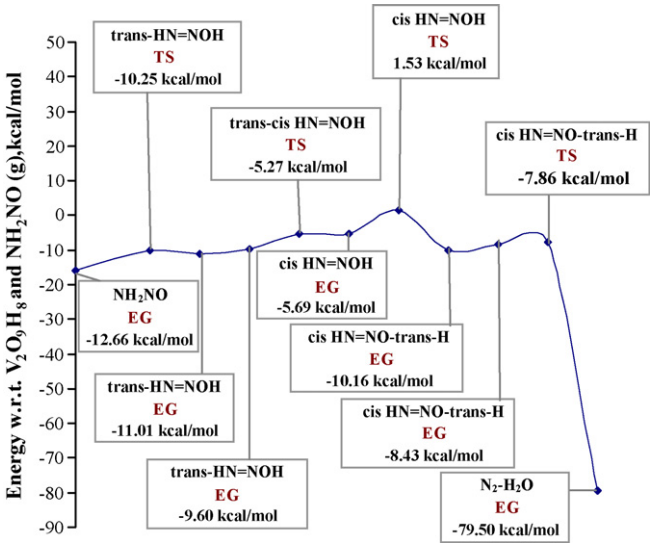

Fig. 7. Potential energy profile for the third part of SCR reaction (TS represents the transition states, while EG stands for the equilibrium geometries).

calculation. The system is taken as neutral and with singlet spin multiplicity in all of the calculations involving this part. The equilibrium geometry of re-adsorbed NH_2NO species having a relative energy of −12.66 kcal/mol is given in Fig. 8. In order to accomplish the decomposition of this product to the final reaction products N_2 and H_2O, a series of many different reaction steps have been energetically investigated and the most favorable reaction path combination involving a push–pull mechanism of hydrogen transfer is obtained. The transition states and equilibrium geometries pertaining to each one of these reaction steps are given separately in Figs. 9–14.

A coordinate driving calculation is first performed by selecting the distance between H4 atom of the nitrosamide species and the O1′ site of the cluster surface as the reaction coordinate. This enables hydrogen transfer to the oxygen atom of the nitrosamide molecule as follows: it is observed by means of the energy profile that as the distance between H4 and O1′ atoms decreases, H1 moves apart from O1 atom. H1 atom is finally captured by the O atom. The transition state

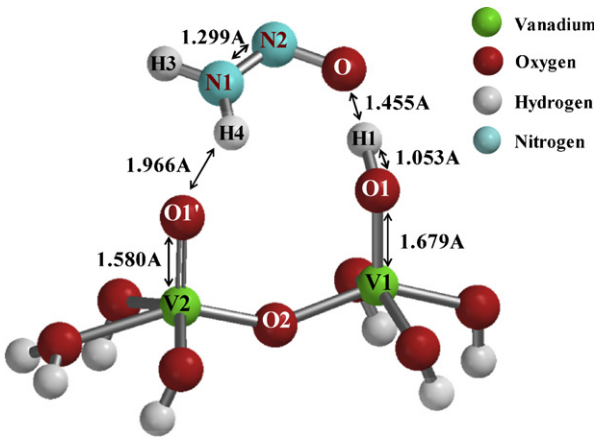

Fig. 8. Equilibrium geometry of nitrosamide species re-adsorbed on a new Brønsted acidic $V_2O_9H_8$ cluster.

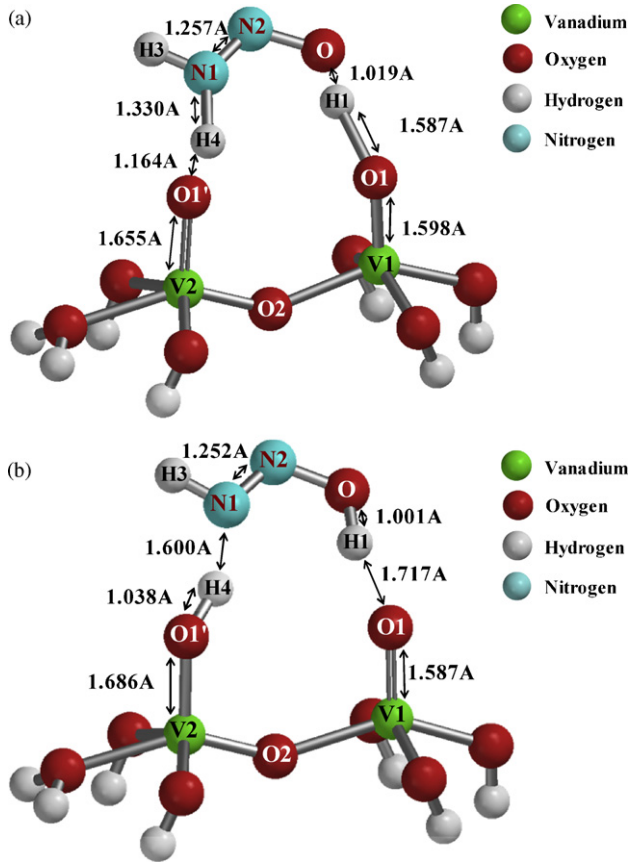

Fig. 9. (a) Transition state geometry and (b) equilibrium geometry structures for *trans*-HN=NOH formation reaction from NH_2NO species.

and equilibrium geometry of this interaction are shown in Fig. 9.

The *trans*-HN=NOH species is further rotated on the cluster surface by a single point equilibrium geometry calculation as given in Fig. 10. At this stage a coordinate driving calculation is employed by selecting a reaction coordinate between O1 and

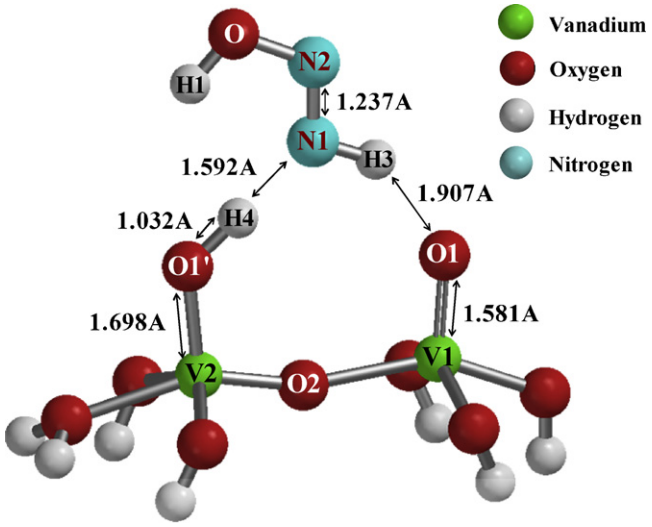

Fig. 10. Equilibrium geometry of the rotated *trans*-HN=NOH species on $V_2O_9H_8$ cluster.

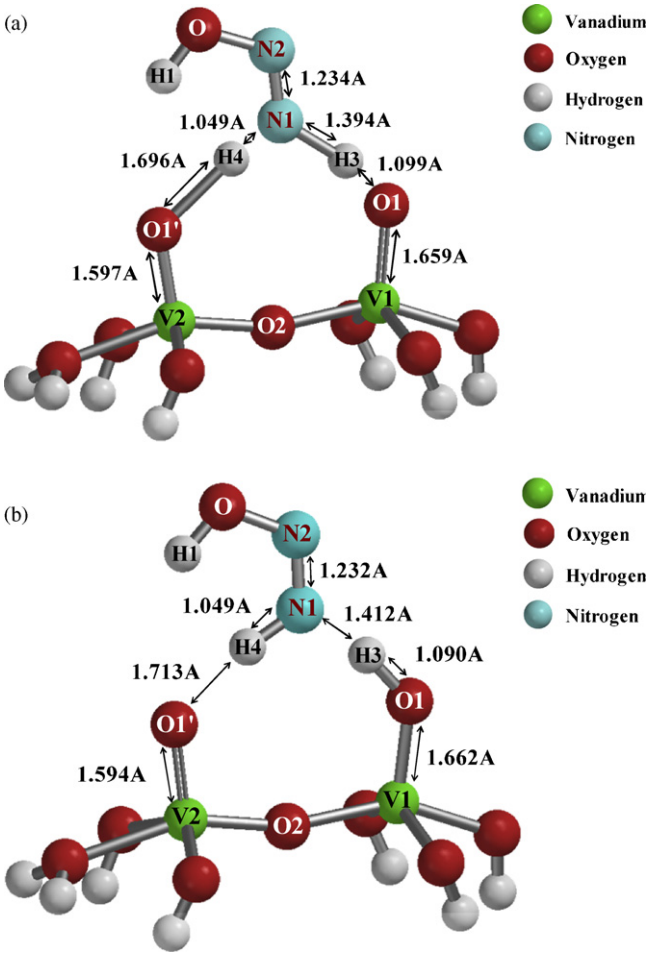

Fig. 11. (a) Transition state geometry for the reaction of formation of *cis*-HN=NOH species from *trans* H-N=NOH species and (b) equilibrium geometry of the adsorbed *cis*-HN=NOH species.

H3 atoms in order to provide *cis*-HN = NOH formation. Using the resultant energy profile, the transition state geometry and equilibrium geometry of this interaction are obtained as shown in Fig. 11. For the transition state geometry, N1–H4 bond is about to be formed as H3 atom of the *trans* H–N=NOH species is about to be captured by V1=O1 site.

The next step for the SCR of NO by NH_3 is the isomerization of the *cis*-HN=NOH species (see Fig. 11(b)) to form *cis*-HN=NO–*trans*-H species. For this purpose N1N2O-H1 dihedral angle is chosen as the reaction coordinate. The transition state and equilibrium geometry obtained accordingly are illustrated in Fig. 12. At the transition state geometry N1N2O-H1 dihedral angle is 77.67° indicating that the H1 atom is about to rotate to form *cis*-HN=NO–*trans*-H species.

Cis-HN=NO–*trans*-H species is rotated again on the cluster in order to take advantage of the hydrogen atom push–pull capability of the catalyst surface (see Fig. 13). A coordinate driving calculation is finally performed for H_2O and N_2 formation reaction by selecting the distance between H3 and O atoms as a decreasing reaction coordinate. The transition state of this interaction having a relative energy difference of −7.86 kcal/mol is illustrated in Fig. 14(a). Searching for the equilibrium geometry of this interaction, it is found that

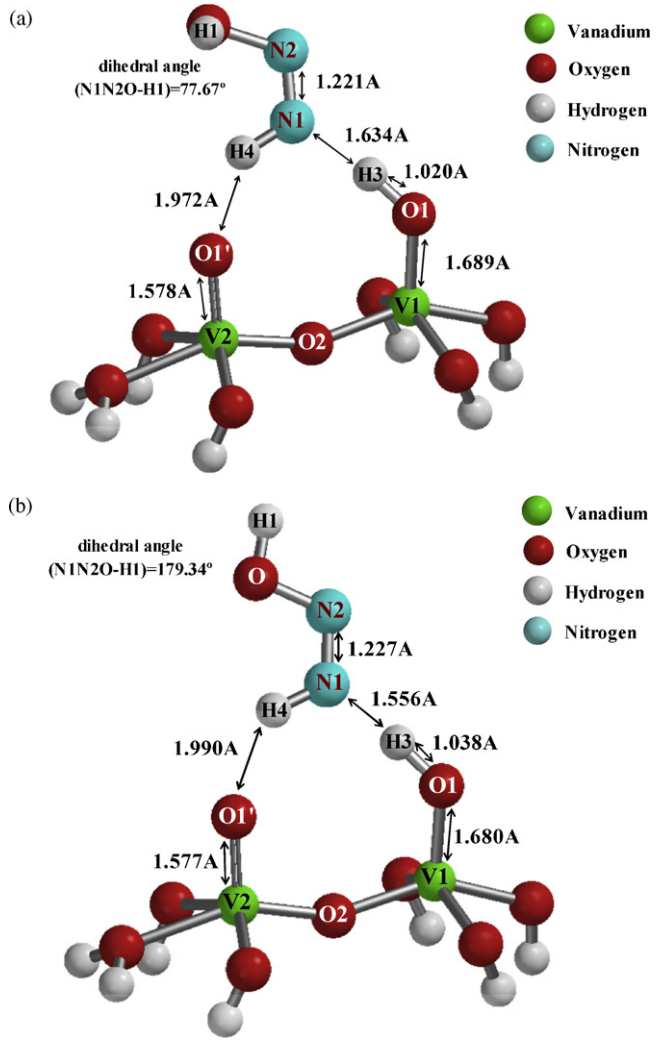

Fig. 12. (a) Transition state geometry for the isomerization reaction of the adsorbed *cis*-HN═NOH species to form *cis*-HN═NO–*trans*-H species and (b) equilibrium geometry of the adsorbed *cis*-HN═NO–*trans*-H species.

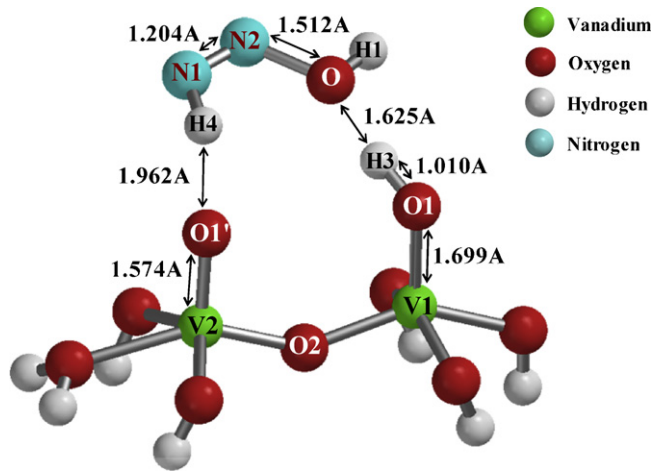

Fig. 13. Equilibrium geometry of the re-adsorbed *cis*-H-N═NO–*trans*-H species on $V_2O_9H_8$ cluster.

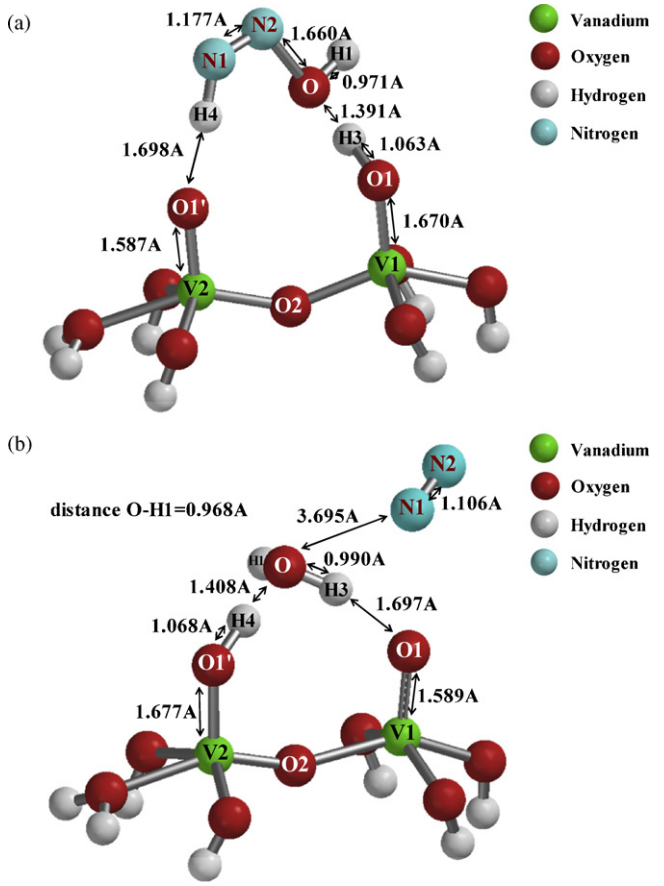

Fig. 14. (a) Transition state geometry and (b) equilibrium geometry for N_2 and H_2O formation reaction from the re-adsorbed *cis*-H-N═NO–*trans*-H species.

formation of water and nitrogen occurs as shown in Fig. 14(b) with a highly exothermic relative energy difference of 79.50 kcal/mol.

3.3.2. *Decomposition of NH_2NO species in gas phase*

As an alternative to the decomposition of NH_2NO species on the cluster surface gas phase decomposition process is considered. The potential energy diagram summarizing the reaction steps of this part is illustrated in Fig. 15 where the relative energy is calculated with respect to the gas phase energy of NH_2NO (g) species. Gas phase decomposition of NH_2NO to reaction products N_2 and H_2O occurs according to the following reaction:

$$NH_2NO \rightarrow H_2O + N_2$$

Before investigating the gas phase decomposition mechanism of NH_2NO into reaction products, the optimized structure for nitrosamide molecule was obtained as given in Fig. 16. Table 2 includes all the bond distance and angle values as well as the NH_2 scissoring and NNH deformation vibration frequency data that are compared with the experimental and theoretical literature values.

In order to yield the reaction products nitrogen and water, NH_2NO molecule must undergo a series of H atom migrations and some isomerization reactions. Therefore, as the first step of the gas phase nitrosamide decomposition reaction, hydrogen

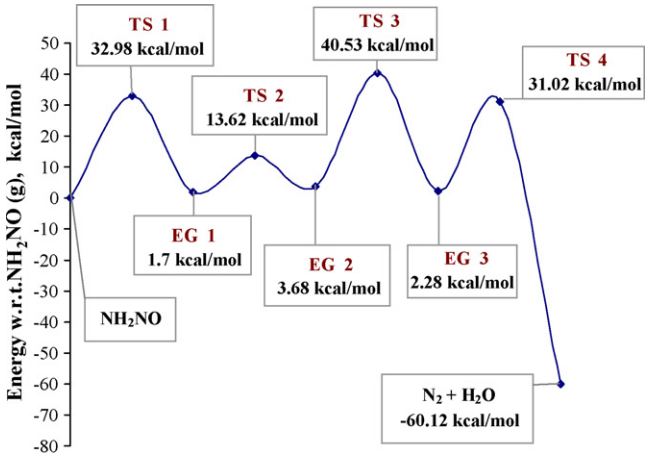

Fig. 15. Potential energy profile for the gas phase NH_2NO decomposition reaction (TS represents the transition states, while EG stands for the equilibrium geometries).

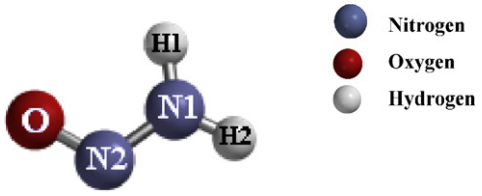

Fig. 16. Optimized geometry of nitrosamide (NH_2NO) molecule.

migration from N1 atom to O atom was investigated. For this purpose a coordinate driving calculation was performed by selecting the distance between O and H1 atoms as reaction coordinate. By means of energy profile obtained for this calculation, the transition state and equilibrium geometry of this interaction are obtained as illustrated in Fig. 17. Here it should be noted that in the calculated vibration frequencies of the transition state structure, there is only one imaginary data (i1498.97 cm^{-1}), representing the migration of H atom from N1 to O atoms.

Table 2
Comparison of the calculated structural parameters (*A* and degree) and vibration frequencies (cm^{-1}) of NH_2NO with theoretical and experimental literature

Geometry	This work		Theoretical literature	
d(N1–N2)	1.336	1.341[a]	1.375[b]	1.307[c]
d(N2–O)	1.221	1.236[a]	1.219[b]	1.186[c]
d(N1–H1)	1.018	1.019[a]	1.022[b]	0.999[c]
d(N1–H2)	1.008	1.010[a]	1.005[b]	0.992[c]
<(N1–N2–O)	113.66	113.0[a]	113.4[b]	114.6[c]
<(H1–N1–N2)	119.34	117.9[a]	114.7[b]	119.4[c]
<(H2–N1–N2)	117.37	115.9[a]	113.4[b]	117.4[c]

Frequencies	Experimental	Theoretical
NH_2 scissoring		
1584 (unscaled)	1521 [39]	1782[c] (unscaled)
1523 (scaled by 0.9613 [35])		1550[c] (scaled by 0.87)
NNH deform.		
1225 (unscaled)	1207 [39]	1392[c] (unscaled)
1178 (scaled by 0.9613 [35])		1211[c] (scaled by 0.87)

[a] MP2 (full)/6-31G* by Aschi et al. [36].
[b] CASSCF/cc-pVDZ by Duan et al. [37].
[c] MP2/6-31** by Harrison et al. [38].

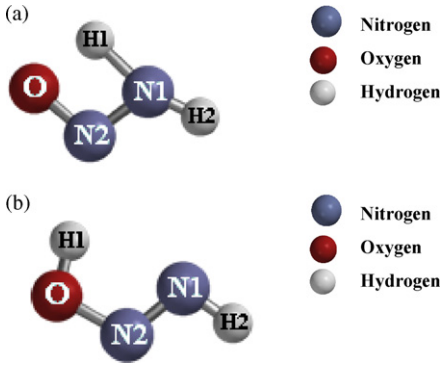

Fig. 17. (a) Transition state and (b) equilibrium geometry for the first H migration reaction of NH_2NO decomposition reaction.

Second step of the NH_2NO decomposition reaction is the isomerization reaction of hydrogen atom (H1) bonded to the oxygen atom. H1 atom in the optimized geometry obtained at the end of the first step has a *trans* conformation with respect to N1N2 bond and a *cis* conformation with respect to ON2 bond. This structure must isomerize to the opposite case in order to let H2 atom migration to O atom for the next steps. For this purpose, isomerization of the H1 atom about O–N2 bond was investigated by means of a coordinate driving calculation for which the dihedral angle between the plane formed by N1–N2–O atoms and H1 atom was selected as the reaction coordinate increasing from 0° to 180° step by step. The transition state and equilibrium geometry obtained by this calculation are given in Fig. 18. The relative energy values obtained here are again in a good agreement with what has been reported in literature (see Table 3).

For the third step of the NH_2NO decomposition reaction, isomerization of H2 atom from *trans* conformation to *cis* conformation about N1N2 bond is considered. Therefore, the angle between N2, N1 and H2 atoms was selected as the reaction coordinate and it was increased from 106° to 286° step by step during the calculation. The transition state and equilibrium geometry obtained accordingly are reported in Fig. 19 For this reaction step, another coordinate driving

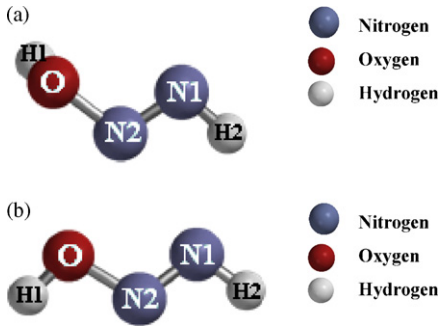

Fig. 18. (a) Transition state and (b) equilibrium geometry for the second step of NH_2NO decomposition, where reaction coordinate is the dihedral angle between the plane of N1–N2–O and H1.

Table 3
Relative energies of transition states (TS) and equilibrium geometries (EG) for each step of the gas phase decomposition of NH_2NO w.r.t. the gas phase total energy of NH_2NO molecule (IG) as compared with other theoretical literature

	Relative energies of the geometries		
	This work[a]	Gilardoni et al. [15][b]	Duan and Page [37][c]
Initial geometry (IG)	0.00	0.00	0.00
TS 1	32.98	32.30	35.14
EG 1	1.70	2.85	−1.36
TS 2	13.62	12.54	9.37
EG 2	3.68	3.67	1.10
TS 3	40.53	35.66	44.49
EG 3	2.28	3.03	0.44
TS 4	31.02	24.20	34.42
Final geometry (FG)	−60.12	−62.47	−72.77

[a] Calculated at B3LYP/6-31G** level.
[b] Calculated at B3LYP/6-311++G** level.
[c] Calculated CASSCF (12-in-11)/cc-pVDZ level.

calculation was also performed by selecting the reaction coordinate as the dihedral angle between the plane formed by O–N1–N2 and the atom H2, where it is decreased from 180° to 0° step by step. However, the energy profile obtained from this calculation gave a higher activation energy barrier of 54 kcal/mol. Relative energy differences for both the equilibrium geometry (EG 3) and the transition state structures (TS 3) agree well with the literature values as compared in Table 3.

For the last step of the gas phase NH_2NO decomposition reaction, an additional coordinate driving calculation, starting from the final geometry of the third step, was carried out selecting the reaction coordinate as the distance between H2 and O atoms for this calculation. By means of the energy profile obtained at the end of this calculation, the transition state and the equilibrium geometry are computed as given in Fig. 20. It clearly indicates the multi-reference electronic state character of the transition state and this result should be considered with care. By considering the relative energy differences of transition state (TS 4) and equilibrium geometry structures, final geometry of SCR (FG), it was concluded that an activation energy of 28.74 kcal/mol is needed for the formation of nitrogen and water products with a heat of formation of −62.4 kcal/mol indicating a highly exothermic reaction. As in

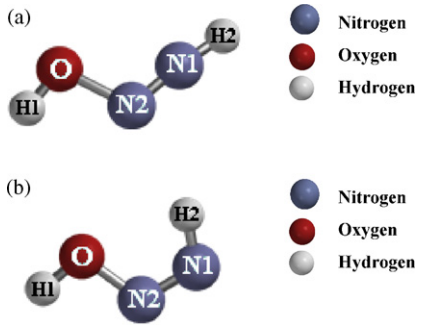

Fig. 19. (a) Transition state and (b) equilibrium geometry for the third step of NH_2NO decomposition.

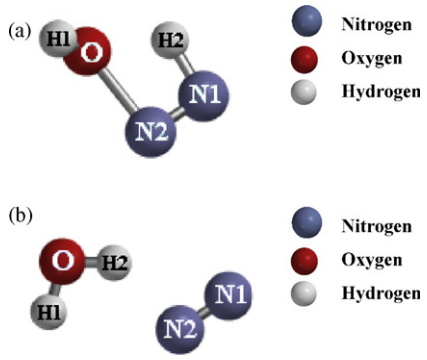

Fig. 20. (a) Transition state and (b) equilibrium geometry for the last step of NH_2NO decomposition reaction.

previous steps, these values agree well with the theoretical literature (see Table 3 for a comparison). As it is the case for the other transition state structures obtained in previous steps, the transition state structure of this step has only one imaginary vibration frequency (i1436.64 cm^{-1}) representing the migration of H2 atom from N1 atom to O atom.

4. Discussion

DFT computations performed lead one to conclude that SCR reaction of NO by ammonia occurs via three main parts. The initiation part includes non-activated Brønsted acidic NH_3 adsorption with an exothermic relative energy of 28.65 kcal/mol. As seen in Fig. 3(a), N1–H3 and N1–H4 bond distances are 1.019 A as the N1–H1 and N1–H2 distances being 1.071 and 1.072 A, respectively, suggesting a symmetrical configuration. The findings in this part are in agreement with what Srnak et al. [40] observed via TPD experiments and what Anstrom et al. [17] and Gilardoni et al. [14] reported by DFT calculations. Srnak et al. [40] estimated the enthalpy for ammonia desorption over Brønsted acidic V–OH site on pure V_2O_5 as between 18 and 26 kcal/mol via TPD experiments. Moreover, Anstrom et al. [17] and Gilardoni et al. [14] calculated the relative energy of the adsorbed NH_3 species over Brønsted acidic V–OH site of the V_2O_5 catalyst as −26 and −25 kcal/mol, respectively. A Mulliken charge value of +0.787e calculated for the equilibrium geometry of the Brønsted acidic NH_3 adsorption reaction suggests that NH_4^+ ion formation occurs at the end of the NH_3 adsorption on Brønsted acidic V–OH site. This result is very close to what Anstrom et al. [17] calculated (+0.808e) and suggests that NH_4^+ ion formation occurs at the end of the NH_3 adsorption on Brønsted acidic V–OH site. Vibration frequency values calculated also provide good agreement with the experimental data for both bending and stretching frequencies of NH_4^+ ion as shown in Table 1. A scaling factor of 1.0873 was obtained through a least squares fit of the experimental data. It should be also noted here that there is no reported theoretical vibration frequency data in the literature with regard to any of the steps of SCR reaction taking place on pure vanadia surface.

The potential energy profile involving the relative energies of species in the second part of SCR reaction (NH_2NO

formation) is illustrated in Fig. 6 together with the initiation part. The rate limiting step of the SCR reaction can be identified as NH_3NHO formation with a high activation barrier of 43.99 kcal/mol. It should be noted that the transition state of this reaction is only an approximate value. However, Anstrom et al. [17] previously reported that the rate limiting step of SCR reaction is the NH_2NO formation reaction from NH_3NHO.

The oxygen sites of the $V_2O_9H_8$ cluster are saturated with the hydrogen atoms with the formation of the nitrosamide species. Hence, a new cluster is employed in the decomposition reactions of this species, and the relative energy values in this part are calculated with respect to the cluster and NH_2NO (g).

In the third part of the SCR reaction, comprising the decomposition of nitrosamide species, the catalytic as well as the gas phase decomposition of this species is considered. Before investigating the gas phase decomposition mechanism of NH_2NO into reaction products, the optimized structure for nitrosamide molecule was obtained as given in Fig. 16. As it is seen in Table 2, all the bond distance and angle values as well as the NH_2 scissoring vibration frequency data show good agreement with the theoretical and experimental values reported in the literature [36–39]. The calculated vibration frequency data of the nitrosamide species are scaled by a factor of 0.9613 which was proposed previously for B3LYP method [35] Disparity observed at the lower vibration frequency of NNH deformation may be due to the anharmonicity present in this system [38].

In order to summarize the energetics of the gas phase decomposition reaction of NH_2NO into nitrogen and water, a potential energy profile is obtained as shown in Fig. 15 by combining relative energy differences of transition and equilibrium geometries of the reaction steps of NH_2NO gas phase decomposition reaction. The relative energy is calculated with respect to the gas phase total energy of NH_2NO. As it is evident from the figure the activation barriers of the reaction steps of the gas phase NH_2NO decomposition are quite high values ranging between 11.92 to 36.85 kcal/mol. On the other hand, the activation barriers for the catalytic decomposition range from 0.57 to 7.22 kcal/mol. Therefore, it is concluded that the gas phase NH_2NO decomposition reaction is energetically a much less favorable reaction in the SCR process as compared to the catalytic decomposition of this species on the cluster surface and the beneficial effect of the vanadia surface providing a push–pull type hydrogen transfer mechanism through oxygen sites is quite apparent in these calculations. The catalytic cycle can then be completed by the oxidation of the V–OH site formed during the last step in part II (NH_2NO formation reactions). A comparison of the SCR reaction species and their relative energy values with the corresponding theoretical literature [17] is given in Table 4. Anstrom et al. [17] performed all of the same reactions on a cluster consisting of four vanadium atoms and calculated the relative energy with respect to the cluster, NH_3 (g) and NO (g). However, in this work NH_2NO decomposition reaction is accomplished on a new $V_2O_9H_8$ cluster and the relative energy values in this part are calculated with respect to the cluster and NH_2NO (g). Moreover in their work, all of the vanadium atoms were kept fixed while in this research, both of the vanadium atoms of the cluster are relaxed. In spite of these important differences the energy profiles obtained are similar. Also the transition state for the isomerization reaction of *cis*-HN=NOH to *cis*-HN=NO–*trans*-H species on the cluster surface has the

Table 4
Comparison of the SCR reaction species and their relative energy values with the corresponding theoretical literature

This work			Anstrom et al. [17]	
Species	Figure	Energy w.r.t. $V_2O_9H_8$, NH_3 (g), NO (g) (kcal/mol)	Species	Energy w.r.t. $V_4O_{16}H_{12}$, NH_3 (g), NO (g) (kcal/mol)
NH_4 EG	Fig. 3	−28.65	NH_4 EG	−26.29
NH_4–NO approximately TS	Fig. 4(a)	15.34	NH_4–NO approximately TS	0.96
NH_3NHO EG	Fig. 4(b)	−2.21	NH_3NHO EG	−5.98
NH_3NHO approximately TS	Fig. 5(a)	16.13	NH_3NHO approximately TS	11.47
NH_2NO EG	Fig. 5(b)	−14.08	NH_2NO EG	−20.79

This work				
Species	Figure	Energy w.r.t. $V_2O_9H_8$, NH_2NO (g), kcal/mol		
NH_2NO EG	Fig. 8	−12.66	NH_2NO EG	−21.99
Trans-HN=NOH TS	Fig. 9(a)	−10.25	*Trans*-HN=NOH approximately TS	−17.45
Trans-HN=NOH EG	Fig. 9(b)	−11.01	*Trans*-HN=NOH EG	−19.60
Trans-HN=NOH EG	Fig. 10	−9.60	*Trans*-HN=NOH EG	−17.21
Trans–cis HN=NOH TS	Fig. 11(a)	−5.27	*Trans–cis* HN=NOH approximately TS	−11.95
Cis HN=NOH EG	Fig. 11(b)	−5.69	*Cis* HN=NOH EG	−12.67
Cis HN=NOH TS	Fig. 12(a)	1.53	*Cis* HN=NOH approximately TS	−6.69
Cis HN=NO–*trans*-H EG	Fig. 12(b)	−10.16	*Cis* HN=NO–*trans*-H EG	−18.16
Cis HN=NO–*trans*-H EG	Fig. 13	−8.43	*Cis* HN=NO–*trans*-H EG	−14.58
Cis HN=NO–*trans*-H TS	Fig. 14(a)	−7.86	*Cis* HN=NO–*trans*-H approximately TS	−13.62
N_2–H_2O EG	Fig. 14(b)	−79.50	N_2–H_2O EG	−65.25

EG, TS, and approximately TS stand for equilibrium geometry, transition state and approximate transition state respectively.

highest activation barrier value of 7.22 kcal/mol among all the steps involved in this part which is again similar to findings by Anstrom et al. [17].

Another important point to be mentioned is that due to the complexity of the reaction, a successful transition state geometry with regard to SCR reaction steps has not yet been reported in the theoretical literature using DFT method. However, in this research the transition state geometries for all of the reaction steps involved were successfully calculated for the third part of the SCR reaction.

It should also be pointed out that nitrosamide species under typical SCR conditions has not yet been reported in the experimental literature. This may be due to very fast decomposition of NH_2NO to the SCR reaction products N_2 and water.

5. Conclusions

The catalytic pathway for the selective catalytic reduction reaction of nitric oxide by ammonia reaction on (0 1 0) $V_2O_9H_8$ cluster surface is studied by means of the density functional theory calculations carried out at B3LYP/6-31G** level. As an initiation reaction, ammonia activation mode over $V_2O_9H_8$ cluster surface was investigated. It is concluded that the SCR reaction is initiated more favorably by the ammonia activation on Brønsted acidic V–OH site, where NH_4^+ ion is formed. This reaction step is calculated to occur through a non-activated process with an exothermic relative energy of 28.65 kcal/mol. These findings are in agreement with previous experimental and theoretical studies. Vibration frequencies are also calculated for the optimized geometry of the Brønsted acidic adsorption reaction and it is found that all the vibration frequencies agree well with what has been observed experimentally in literature. For the second part of the SCR reaction that involves the interaction of NO with the ammonia adsorbed cluster, reaction steps leading to the formation of NH_3NHO adduct and NH_2NO species take place sequentially. NH_3NHO formation having an activation barrier of 43.99 kcal/mol turns out to be the rate limiting step of the SCR reaction. In the third part, catalytic as well as the gas phase decomposition reactions of NH_2NO species into N_2 and H_2O are considered and the findings of this part are in accordance with the theoretical literature. The reaction steps on the cluster surface involve a push–pull type transfer of the H atoms between the species formed and the V=O and V–OH sites of the cluster surface. It is found that the activation barriers of the NH_2NO decomposition on the cluster surface are much lower than those calculated for gas phase reactions alone. Hence, catalytic nitrosamide decomposition is found to be more favorable than gas phase decomposition of this species. The catalytic cycle of the SCR reaction can be completed by the oxidation of the V–OH site formed during the last step of this part.

References

[1] M. Inomata, A. Miyamoto, Y. Murakami, J. Catal. 62 (1980) 140.
[2] M. Inomata, A. Miyamoto, Y. Murakami, J. Phys. Chem. 85 (1981) 2372.
[3] F.J.J.G. Janssen, F.M.G. van den Kerkhof, H. Bosch, J.R.H. Ross, J. Phys. Chem. 91 (1987) 5921.
[4] F.J.J.G. Janssen, F.M.G. van den Kerkhof, J. Phys. Chem. 91 (1987) 6633.
[5] N.-Y. Topsøe, J. Catal. 128 (1991) 499.
[6] N.-Y. Topsøe, H. Topsøe, J.A. Dumesic, J. Catal. 151 (1995) 226.
[7] N.-Y. Topsøe, H. Topsøe, J.A. Dumesic, J. Catal. 151 (1995) 241.
[8] M.G. Gasior, J. Haber, T. Machej, T. Czeppe, J. Mol. Catal. 43 (1988) 359.
[9] U.S. Ozkan, Y. Cai, M.W. Kumthekar, J. Catal. 149 (1994) 375.
[10] U.S. Ozkan, Y. Cai, M.W. Kumthekar, J. Catal. 149 (1994) 390.
[11] G. Ramis, L. Yi, G. Busca, M. Turco, E. Kotur, R.J. Willey, J. Catal. 157 (1995) 523.
[12] G. Ramis, L. Yi, G. Busca, Catal. Today 28 (1996) 373.
[13] G. Busca, L. Lietti, G. Ramis, F. Berti, Appl. Catal. B 18 (1998) 1.
[14] F. Gilardoni, J. Weber, A. Baiker, Inter. J. Quan. Chem. 61 (1997) 683.
[15] F. Gilardoni, J. Weber, A. Baiker, J. Phys. Chem. A 101 (1997) 6069.
[16] M. Anstrom, N.-Y. Topsøe, J.A. Dumesic, Catal. Lett. 78 (1–4) (2002) 281.
[17] M. Anstrom, N.-Y. Topsøe, J.A. Dumesic, J. Catal. 213 (2003) 115.
[18] X. Yin, H. Han, A. Miyamoto, Phys. Chem. Chem. Phys. 2 (2000) 4243.
[19] N.A. Kachurovskaya, E.P. Mikheeva, G.M. Zhidomirov, J. Mol. Catal. A 178 (2002) 191.
[20] E.P. Mikheeva, N.A. Kachurovskaya, G.M. Zhidomirov, Kin. Catal. 43 (2002) 223.
[21] Y. Izumi, F. Kiyotaki, H. Yoshitake, K. Aika, T. Sugihara, T. Tatsumi, Y. Tanizawa, T. Shido, Y. Iwasawa, Chem. Commun. (2002) 2402.
[22] N.U. Zhanpeisov, S. Higashimoto, M. Anpo, Inter. J. Quan. Chem. 84 (2001) 677.
[23] K. Jug, T. Homann, T. Bredow, J. Phys. Chem. A 108 (2004).
[24] W. Kohn, L.J. Sham, Phys. Rev. 140 (1965) A1133.
[25] M.T.M. Koper, R.A. van Santen, J. Electroanal. Chem. 472 (1999) 126.
[26] R.A. van Santen, M. Neurock, Catal. Rev.-Sci. Eng. 37 (1995) 557.
[27] A.D. Becke, Phys. Rev. B 38 (1988) 3098.
[28] A.D. Becke, M.R. Roussel, Phys. Rev. A 39 (1989) 3761.
[29] C. Lee, W. Yang, R.G. Parr, Phys. Rev. B 37 (1988) 785.
[30] W. Hehre, L.D. Burke, A.J. Shusterman, A Spartan Tutorial, Wavefunction, Inc., Irvine, CA, 1993.
[31] Spartan'02 Windows, Tutorial and User's Guide, Wavefunction, Inc., Irvine CA, 2001.
[32] A. Michalak, M. Witko, K. Hermann, Surf. Sci. 375 (1997) 385.
[33] K. Hermann, M. Witko, R. Druzinic, Faraday Discuss. 114 (1999) 53.
[34] K. Hermann, M. Witko, R. Druzinic, A. Chakrabarti, B. Tepper, M. Elsner, A. Gorschlüter, H. Kuhlenbeck, H.J. Freund, J. Elect. Spec. Relat. Phen. 98–99 (1999) 245.
[35] M.W. Wong, Chem. Phys. Lett. 256 (1996) 391.
[36] M. Aschi, F. Grandinetti, Chem. Phys. Lett. 267 (1997) 98.
[37] X. Duan, M. Page, J. Mol. Str. (Theochem.) 333 (1995) 233.
[38] J.A. Harrison, R.G.A.R. Maclangan, A.R. Whyte, Chem. Phys. Lett. 130 (1986) 98.
[39] I.N. Crowley, J.R. Sodeau, J. Phys. Chem. 94 (1990) 8103.
[40] T.Z. Srnak, J.A. Dumesic, B.S. Clausen, E. Törnqvist, N.-Y. Topsøe, J. Catal. 135 (1992) 246.